Electronic Supplementary Information

Intercalation of Bi nanoparticles into graphite enables ultra-fast and ultra-stable anode material for Sodium-ion batteries

Ji Chen,[†,1] *Xiulin Fan,*[†,1] *Xiao Ji,*[1] *Tao Gao,*[1] *Singyuk Hou,*[1] *Xiuquan Zhou,*[2] *Luning Wang,*[2] *Fei Wang,*[1] *Chongyin Yang,*[1] *Long Chen,*[1] *and Chunsheng Wang**[,1]

[1]Department of Chemical and Biomolecular Engineering, University of Maryland, College Park, MD 20742, USA. E-mail: cswang@umd.edu

[2]Department of Chemistry and Biochemistry, University of Maryland, College Park, MD 20742, USA.

Experimental Section

Chemicals.

Bismuth powder (−100 mesh, 99% trace metals basis), Potassium chunks (in mineral oil), 98% trace metals basis, were purchased from Sigma-Aldrich. Natural graphite flakes (Type 3243) was provided by Asbury Carbons. All the reagents were used as received without purification.

Synthesis of K_3Bi alloy.

In a typical experiment, 0.7 g potassium and 1.3 g bismuth were added into a one-end-sealed quartz tube with inner diameter of 8 mm in a glove box filled with Argon. Then the other end of the tube was sealed under vacuum, and this tube was further

sealed into another quartz tube with larger inner diameter under vacuum. The as-sealed double ampule was transferred into tube furnace and ramped to 550 ^{o}C in 100 min and kept at this temperature for 2 h then cool down to room temperature.

Synthesis of $KBi_{0.6}C_8$

The as-prepared K_3Bi alloy was ground and well mixed with graphite and bismuth. Similarly, this mixture was sealed in double ampule, and ramped to 550 ^{o}C in 100 min and kept at this temperature for 24 h then cooled down to room temperature.

Conversion of $KBi_{0.6}C_8$ to Bi@Graphite

The as-prepared $KBi_{0.6}C_8$ and remaining KBi alloy was ground to fine powders using mortar and pestle. Afterwards, the powders were slowly added into ethanol and stirred overnight to chemically de-intercalate the potassium from $KBi_{0.6}C_8$ and react with outside KBi alloy. The ethanol-washed powders were filtered, washed with ethanol, and dried. Successively, the ethanol-washed powders were washed by diluted HNO_3 (1:3 weight dilution by water) to remove the outside Bi, while the intercalated Bi nanoparticle still reserved since HNO_3 cannot penetrate into graphite, which is substantially different from Bi@rGO composites. Finally, the HNO_3-washed powders were stirred in diluted HCl solution and filtered to remove adsorbed Bi (III) species. The Bi@Graphite is obtained after drying the HCl-washed powders.

Material Characterizations

Scanning electron microscopy (SEM) and transmission electron microscopy (TEM) images were taken by Hitachi SU-70 analytical SEM (Japan) and JEOL (Japan)

2100F field emission TEM, respectively. Powder X-ray diffraction (PXRD) data were collected on a Bruker D8 X-ray diffractometer using Cu Kα radiation (λ = 1.5418 Å). Raman measurements were performed on a Horiba Jobin Yvon Labram Aramis using a 532 nm diode-pumped solid-state laser, attenuated to give ~ 900 μW power at the sample surface.

Determination of Bi content in Bi@Graphite

The amount of Bi in Bi@Graphite was determined based on the weight of the Bi determined by ICP-AES. The Bi@Graphite was heated in air to 800 ^{o}C to remove the graphite sheath and the remaining yellow Bi_2O_3 was dissolved into nitric acid. The mass ratio of Bi in the Bi@Graphite composite is ca. 30 wt%.

Electrochemical Measurements

The electrochemical tests were performed using a coin-type half cell (CR 2032). Metallic sodium was used as the counter and reference electrode. To prepare the working electrode, the as-synthesized Bi@Graphite, carbon black, and sodium alginate with mass ratio 8:1:2 were hand milled with water into a homogeneous slurry using a pestle and mortar. The slurry mixture was coated onto Cu foil (active material ~0.5 mg/cm^2) and then dried at 90 ºC for 12 h under vacuum. Although the relatively low loadings are inappropriate for real batteries, they are commonly used in the testing of high-rate electrode. Similar active material loading used here is to compare the rate performance with previous reported materials. The electrolyte solution was comprised of 1 M $NaPF_6$ in DME. The cells were assembled with a polypropylene

(PP) microporous film (Celgard 3501) as the separator. Electrochemical performance was tested using Arbin battery test station (BT2000, Arbin Instruments, USA). Capacities were calculated based on the total mass of Bi@Graphite composite. Cyclic voltammogram scanned at different rates between 0 and 1.8 V was recorded using a CHI 600E electrochemical workstation (CH Instruments Inc. USA).

Discussion on the Process and Mechanism of Preparation of Metal@Graphite

Intercalation of Metal Alloys into Graphite

Among the ternary GICs, those of particular interest are the ternary graphite intercalation compounds (t-GIC) with the metal alloys intercalated in multiple layers. The metal alloys usually contain a metal which easily intercalates in its pure state (electropositive alkali metals such as K, Rb, and Cs, denoted as M) and a metal which barely intercalates by itself (less electropositive metals such as Hg, Tl, and Bi, denoted as N). Upon contact with the melting alloy of M and N, graphite is intercalated. This is the only known way to introduce less electropositive metals N into interlayers in graphite. The structure of as-prepared t-GIC is demonstrated in Fig. 1, which indicates G-M-N-M-G repeating unit in which metal alloys are in the form of triple layer.

It should also be noted that the molar fraction of alkali metal M to less electropositive metal N is important to determine the products of the reaction between metal alloys and graphite.

i) If the M molar fraction is too low, no intercalation occurs.

ii) If the M molar fraction is too high, M will intercalate by itself.

iii) For intermediate values of molar fraction, t-GIC is the product.

Choice of Metal Alloy

Intercalation of alloys into graphite is exothermal and the formed GIC decomposes or deintercalates above a certain temperature. To achieve the low stage (stage 1 or 2) GIC, the melting temperature of the alloy should be lower than the equilibrium temperature of low stage GIC. In our case, metal N must be chosen from those electrochemically active as anode materials for batteries. Considering both the melting temperature and composition of the metal alloys by reviewing phase diagram, we choose the K-Bi system as a demonstration.

Transformation of t-GIC to Metal@Graphite

The synthesis of binary metal graphite GIC by reacting graphite with less electropostive metal N alone has never been successful. However, with the help of an electropositive alkali metal M, less electropostive metal N can be intercalated in between graphene layers in graphite, forming t-GIC. Successive hydrolyzation of the t-GIC with protic solvent can result in the deintercalation of electropositive alkali metal M, with less electropostive metal N remains inside graphite. This phenomenon has been previously reported for synthesis of Hg graphite compound.[1]

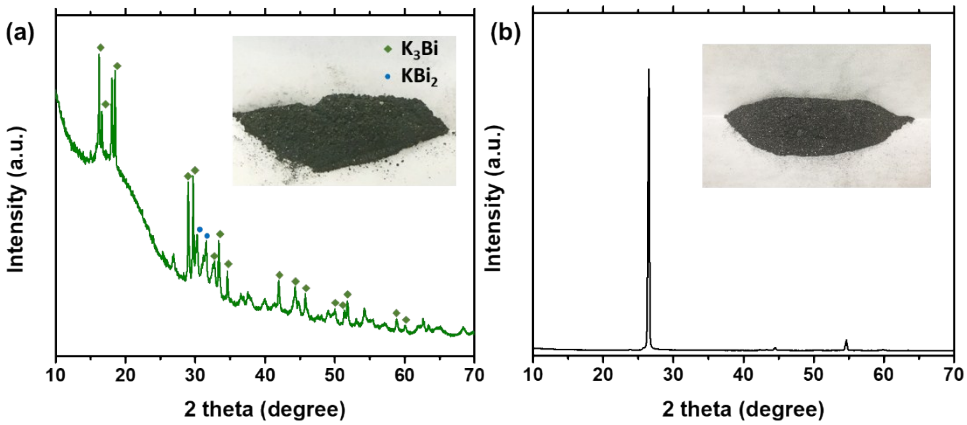

Figure S1. XRD patterns of (a) as-prepared K_3Bi alloy and (b) graphite type 3243. The insets show the photos of the powder samples, respectively.

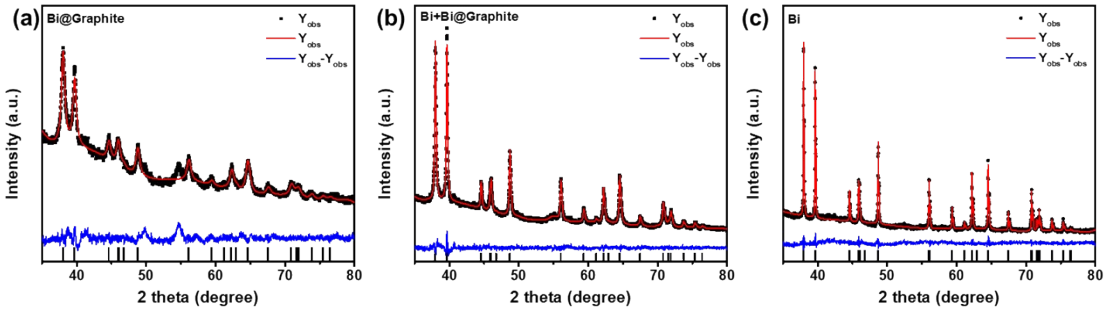

Figure S2. XRD patterns and corresponding Rietveld refinements of (a) Bi@Graphite, (b) Bi+Bi@Graphite, and (c) Bi.

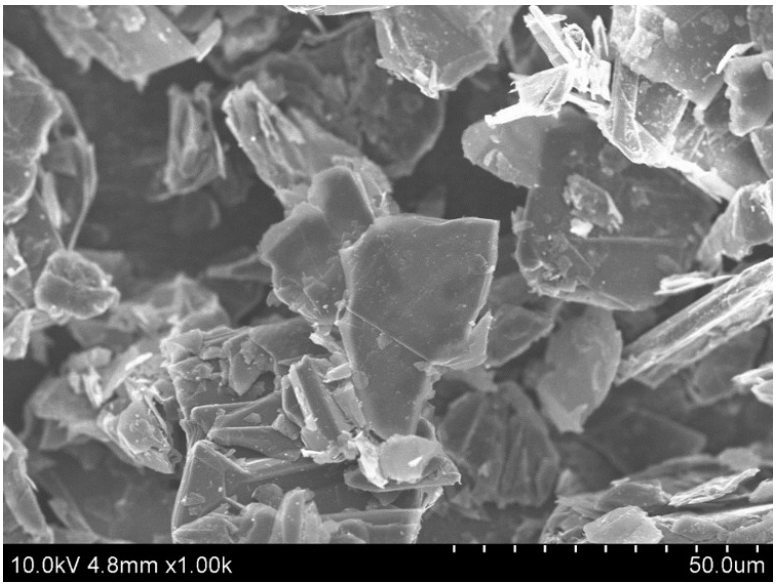

Figure S3. SEM image of graphite particle.

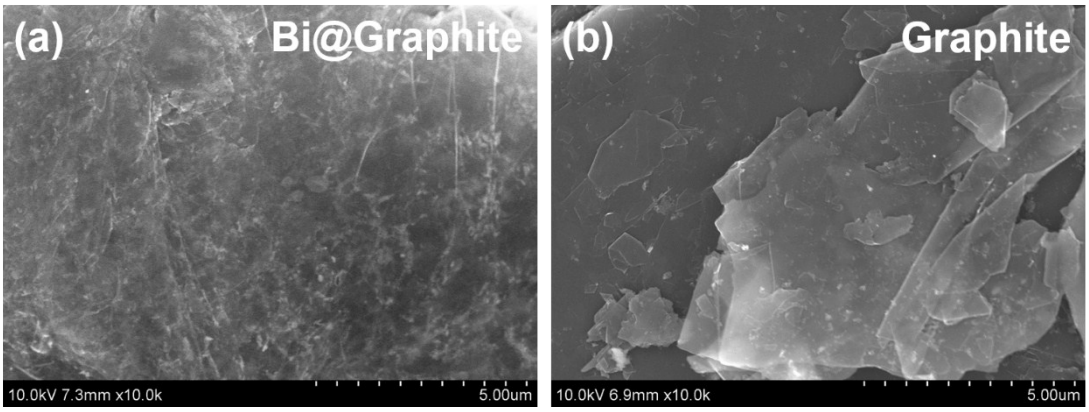

Figure S4. SEM images of (a) Bi@Graphite and (b) graphite

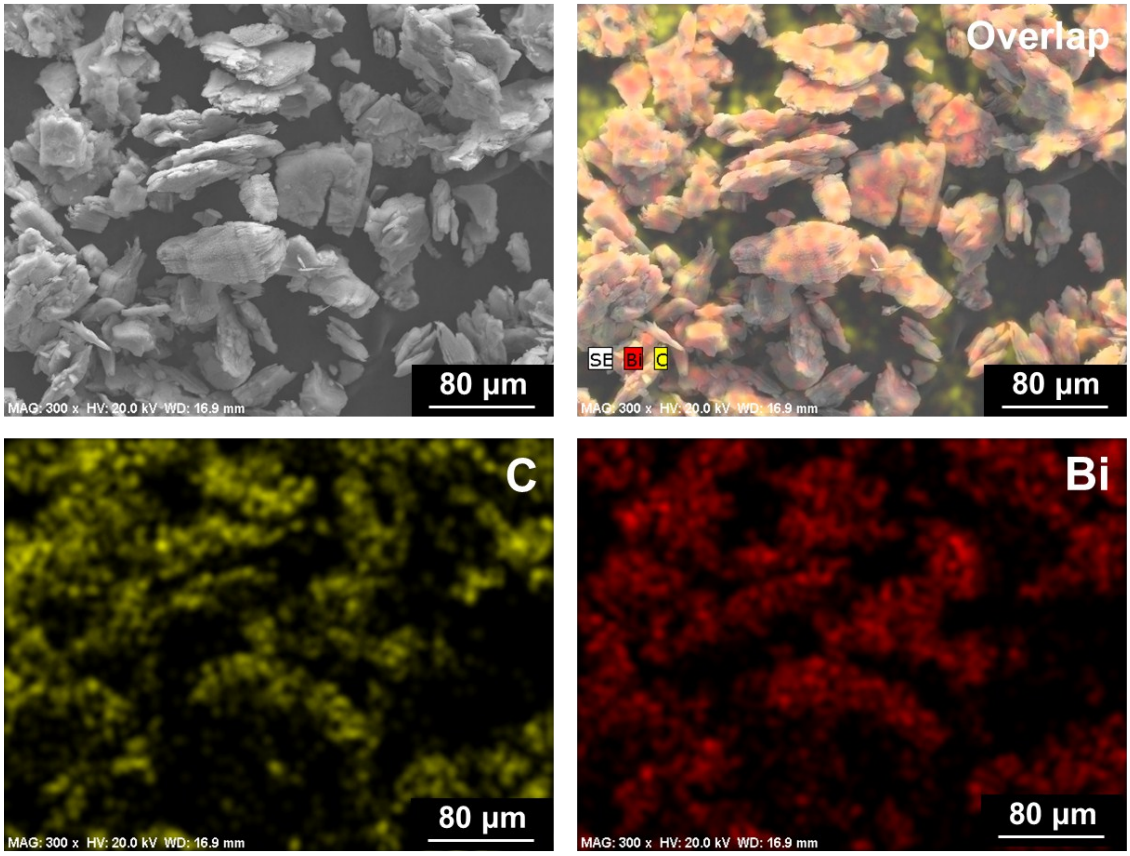

Figure S5. SEM image and corresponding C, Bi, and overlapped elemental mapping images of Bi@Graphite

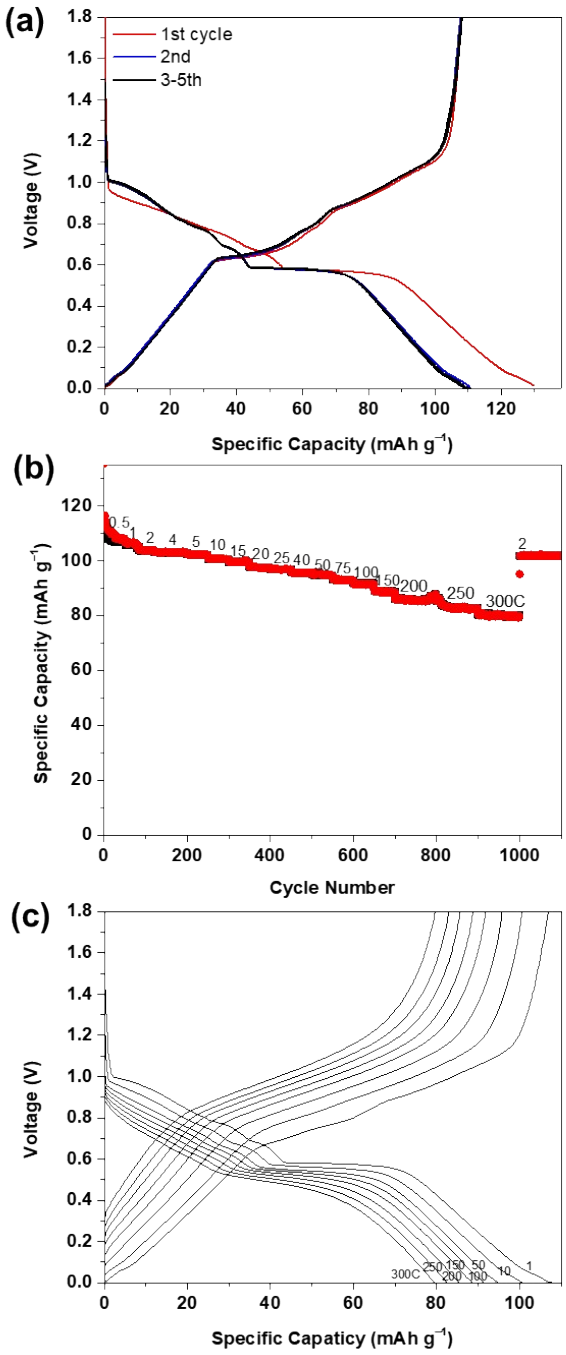

Figure S6. (a) Galvanostatic charge/discharge curves of graphite at a constant current of 55 mA g^{-1} in the voltage window 0.01-1.8 V at room temperature; (b) rate capability at different charge/discharge rates; (c) voltage-capacity curves at different rates (increased from 1C to 300C).

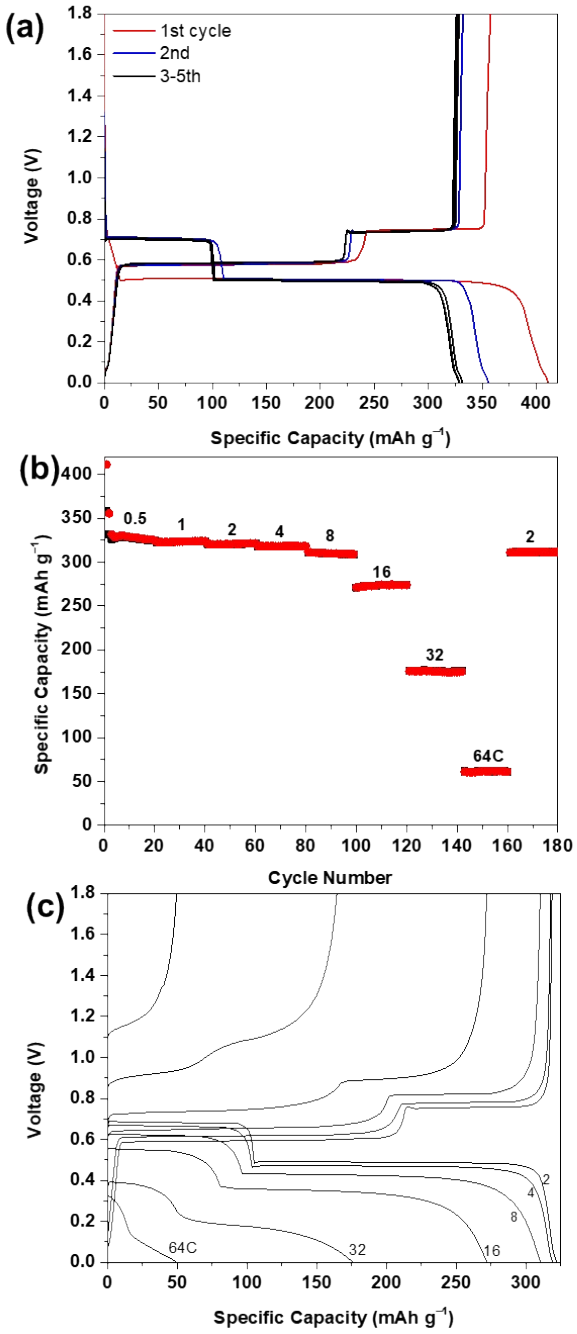

Figure S7. (a) Galvanostatic charge/discharge curves of Bi at a constant current of 165 mA g^{-1} in the voltage window 0.01-1.8 V at room temperature; (b) rate capability at different charge/discharge rates; (c) voltage-capacity curves at different rates (increased from 1C to 64C).

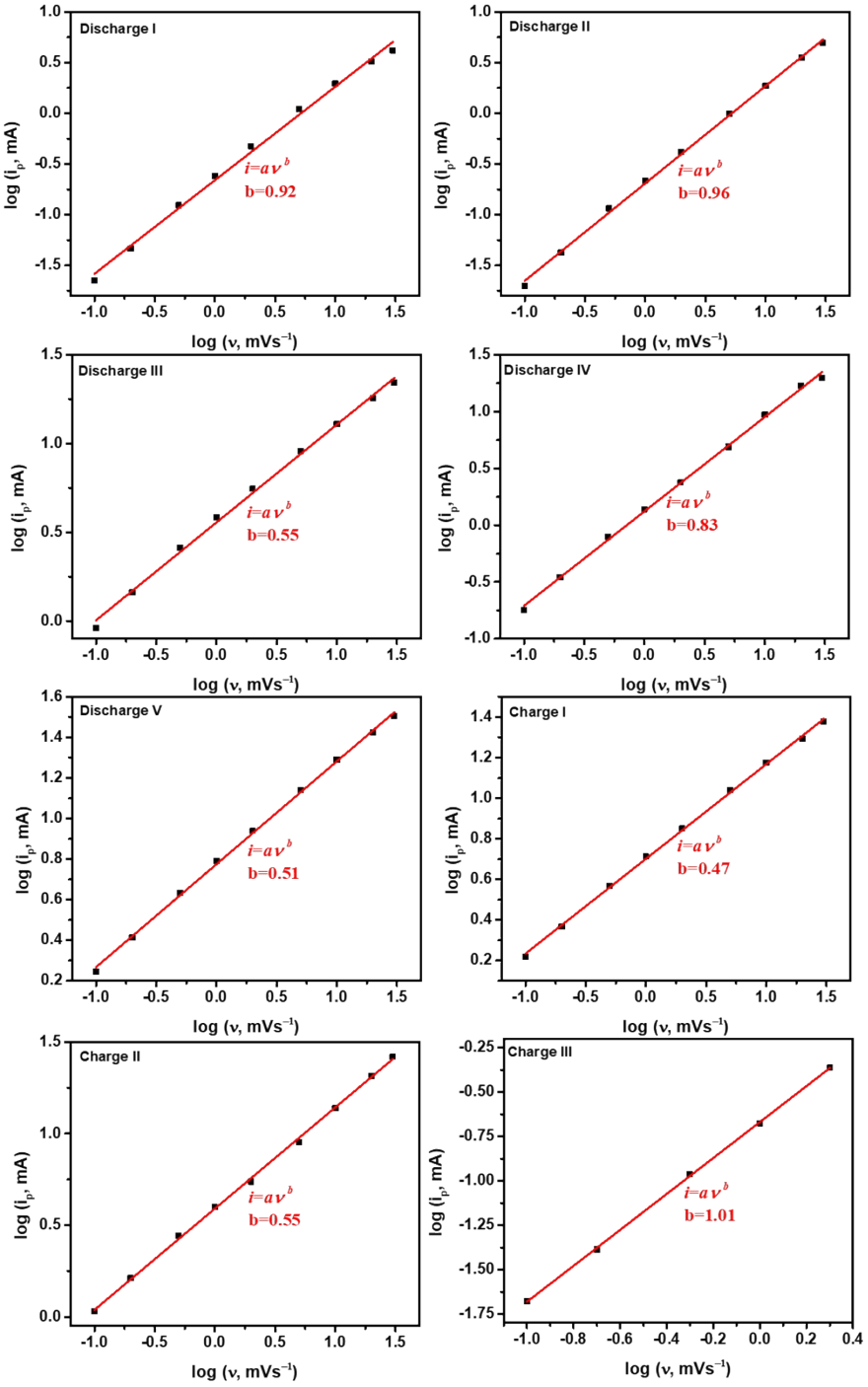

Figure S8. Log i (peak current) vs log υ (scan rate) plots at charging/discharging from the CV curves of Bi@Graphite.

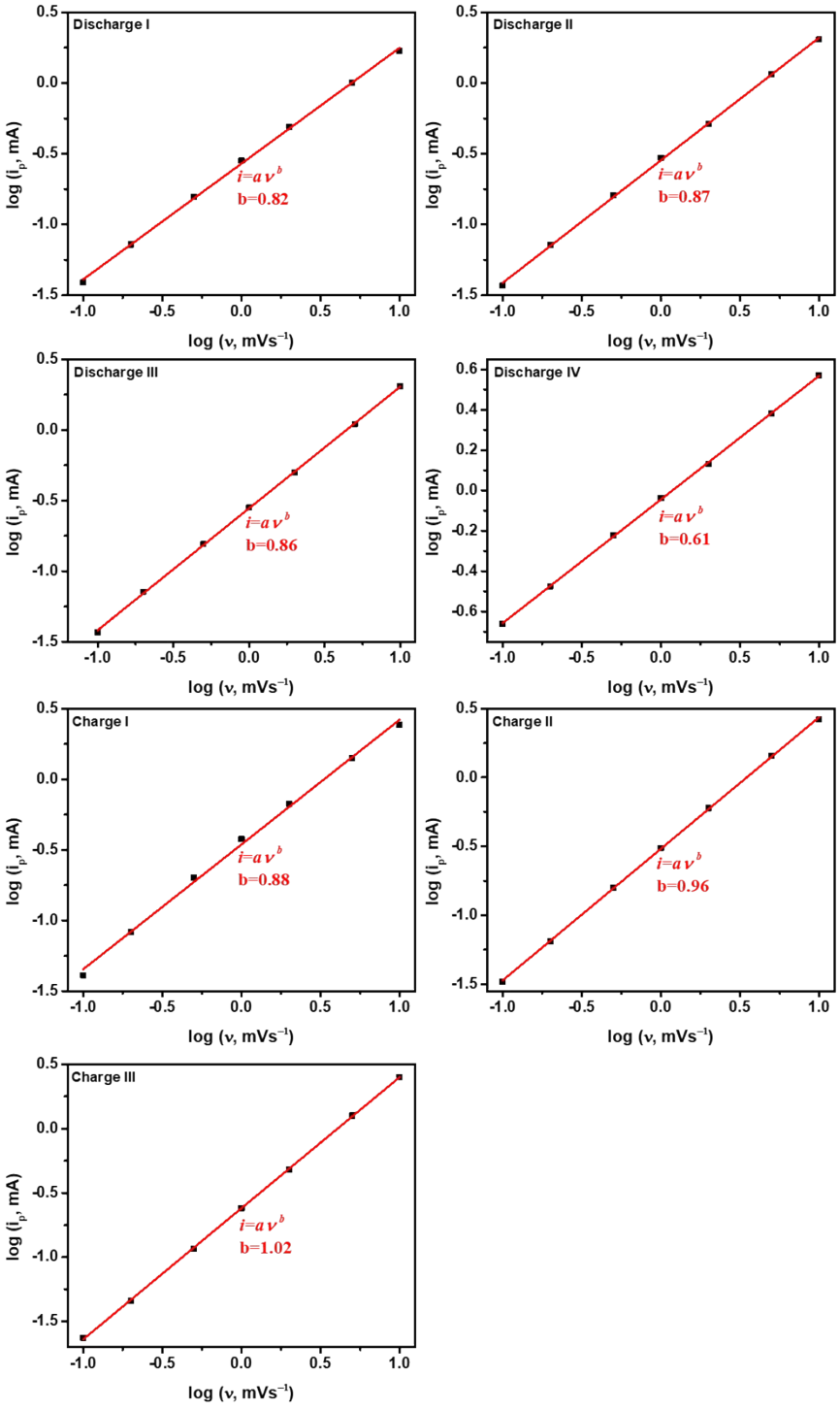

Figure S9. Log i (peak current) vs log υ (scan rate) plots at charging/discharging from the CV curves of graphite.

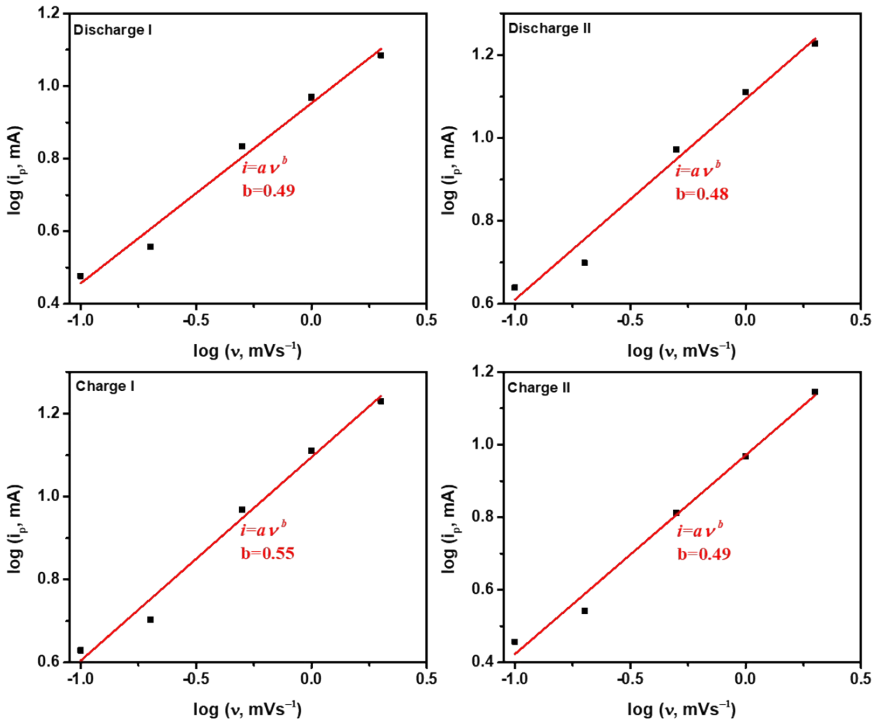

Figure S10. Log i (peak current) vs log υ (scan rate) plots at charging/discharging from the CV curves of Bi electrode.

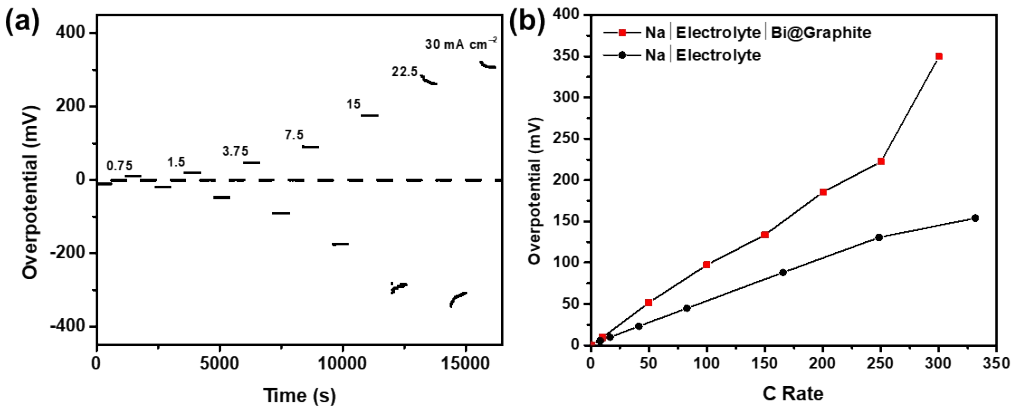

Figure S11. (a) Overpotential vs time at different current densities in Na||Na symmetric cell; (b) comparison of overpotential between Na|Electrolyte and Na|Electrolyte|Bi@Graphite.

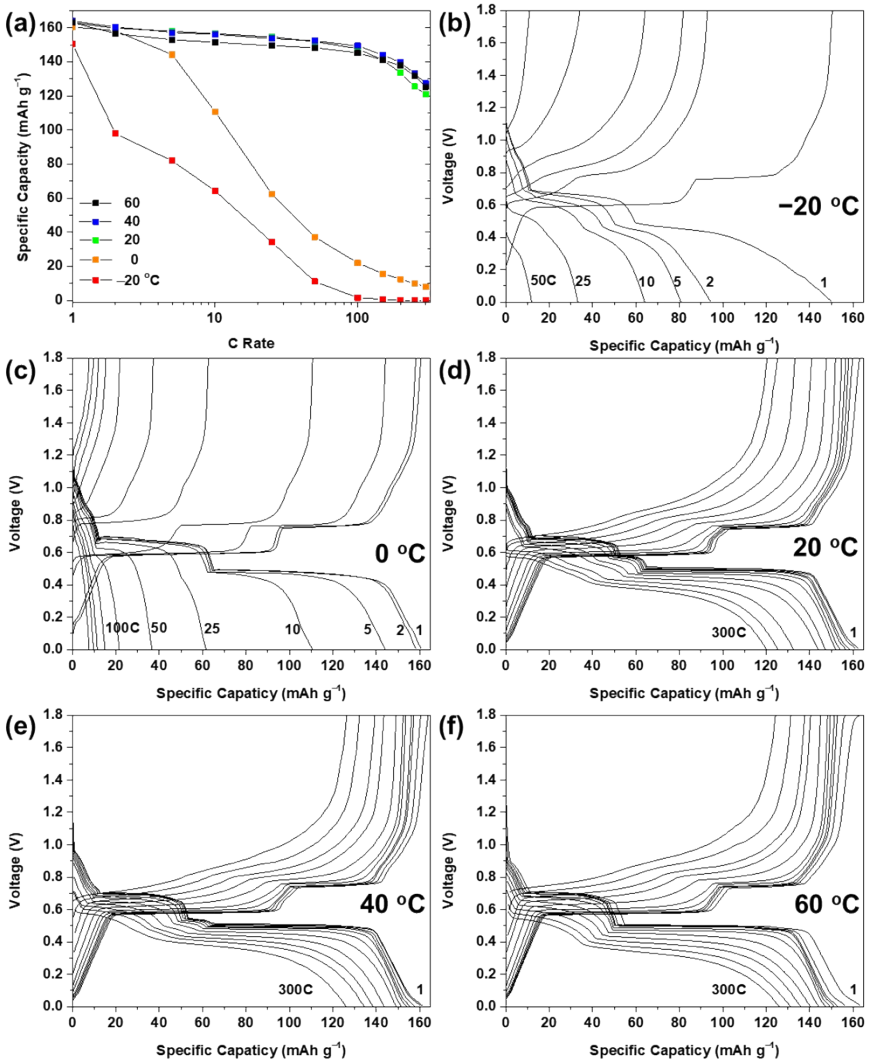

Figure S12. (a) Rate capability of Bi@Graphite composite at different temperatures; (b-f) voltage-capacity curves at different rates (1, 2, 5, 10, 25, 50, 100, 150, 200, 250, and 300C, the temperature is denoted in each panel.)

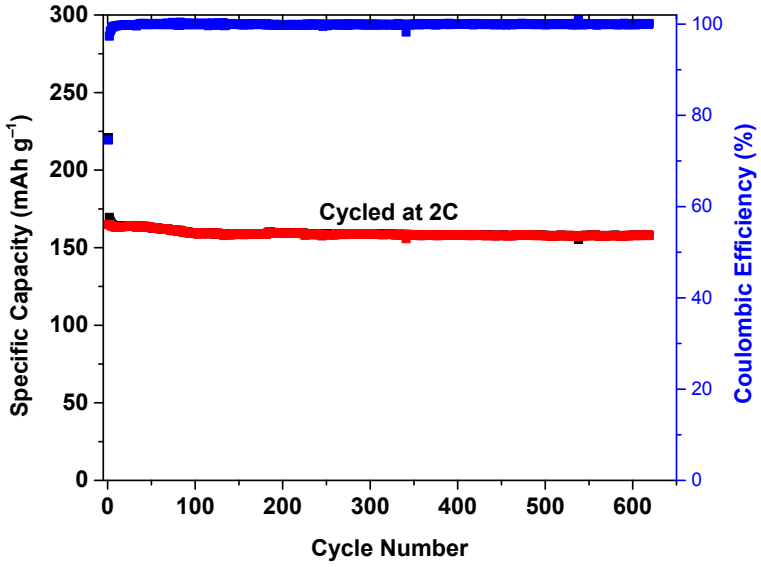

Figure S13. Stability test of Bi@Graphite anode at 2C after 20 cycles at 0.5C.

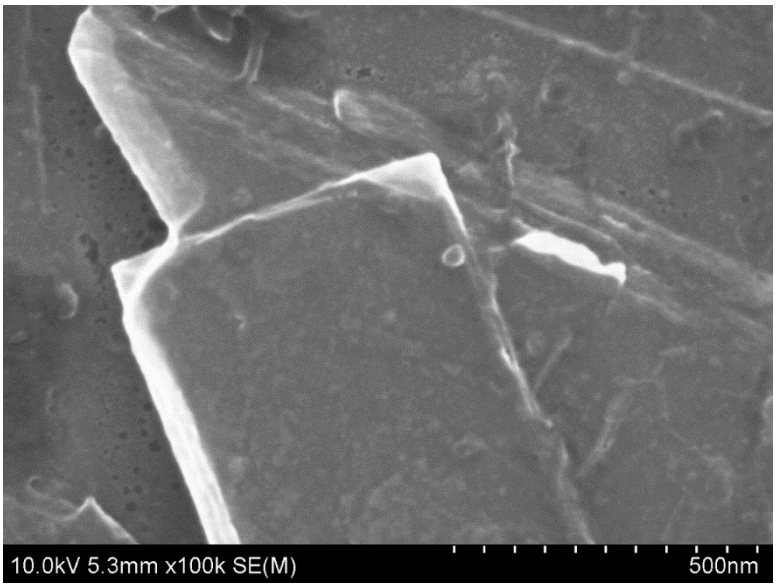

Figure S14. SEM images of Bi@Graphite after cycling for 100 cycles.

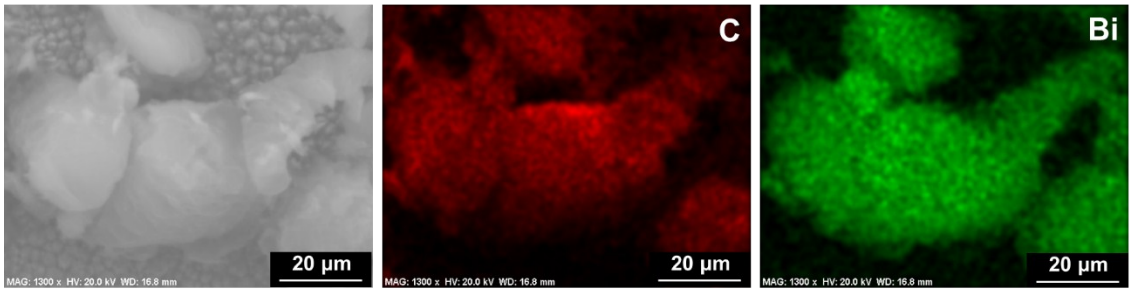

Figure S15. SEM image and corresponding C, Bi elemental mapping images of Bi@Graphite electrode.

1. M. Rabinovitz, H. Selig and J. Levy, *Angew. Chem. Int. Edit.*, 1983, **22**, 53-53.